frontiers in Earth Science

ORIGINAL RESEARCH
published: 20 May 2021
doi: 10.3389/feart.2021.615208

Geochemical and Petrographic Characterization of Marine-Continental Transitional Facies Shale (Qilian Basin, China): Origin of Organic Matter Input, Depositional Environments and Hydrocarbon Generation Potential

Guocang Wang[1†], Minzhuo Sun[1†], Zongwang Yi[2], Li Zhou[3], Jie Ye[4] and Heyong Tan[5]*

[1] Northwest Institute of Eco-Environment and Resources, Chinese Academy of Sciences, Lanzhou, China, [2] Chongqing Geological and Mineral Resource Exploration and Development Bureau 107 Geological Team, Chongqing, China, [3] PetroChina Qinghai Oilfield Research Institute of Exploration & Development, Dunhuang, China, [4] Henan Aero Geophysical Survey and Remote Sensing Center, Zhengzhou, China, [5] Henan Institute of Geological Survey, Zhengzhou, China

This study, for the first time, investigates the source, keroger pattern, evolution degree, sedimentary environment, and evaluates the hydrocarbon generating ability of marine-continental transitional facies shale from the Ebao area of the Qilian Basin in western China. The organic-rich shales of the marine-continental transitional facies were subjected to total organic carbon (TOC), rock pyrolysis, the biomarkers and kerogen microscopy analyses. The kerogen microscopy analyses indicated that the sample from ZK001 well and ZK2002 well had a mass of vitrinite and small number of exinite, so kerogen type was mainly humic. According to vitrinite reflectance, the organic matter was in the stage of maturity to high maturity. The organic analyses indicated that the shale samples possessed the features of the higher TOC and a mixed of terrestrial and marine sources and maturity to high maturity. These features were compatible with the characterized of kerogen microscopy characteristics. A lot of organic materials in the studied shales form ZK001 well and ZK2002 well could be because there were fine protection under salt lake facies and hypoxic marine environment. Therefore, the studied shales of marine-continental transitional facies shale had very good hydrocarbon generating ability as a result of the existence of a lot of high maturity organic materials of humic.

Keywords: Qilian Basin, shales, biomarkers, marine-continental transitional facies, hydrocarbon-generating potential

OPEN ACCESS

Edited by:
Zhilei Sun,
Qingdao Institute of Marine Geology (QIMG), China

Reviewed by:
Attilio Sulli,
University of Palermo, Italy
Xiaofeng Wang,
Northwest University, China

****Correspondence:***
Minzhuo Sun
sunminzhuo@nieer.ac.cn

† These authors have contributed equally to this work and share first authorship

Specialty section:
This article was submitted to Geochemistry, a section of the journal Frontiers in Earth Science

Received: *08 October 2020*
Accepted: *08 April 2021*
Published: *20 May 2021*

Citation:
Wang G, Sun M, Yi Z, Zhou L, Ye J and Tan H (2021) Geochemical and Petrographic Characterization of Marine-Continental Transitional Facies Shale (Qilian Basin, China): Origin of Organic Matter Input, Depositional Environments and Hydrocarbon Generation Potential. Front. Earth Sci. 9:615208. doi: 10.3389/feart.2021.615208

INTRODUCTION

The main shale gas reservoir develops in organic-rich shale of marine, continental, and marine-continental transitional facies in China (Li et al., 2009; Zou et al., 2010; Li C. W. et al., 2015). At present, the shale gas that has been developed on a large scale were the marine shale gas, such as the hundreds of billions of cubic natural gas in Fuling and Weiyuan area, the trillion cubic of natural gas in southern Sichuan and other regions (Dai et al., 2020). Compared with marine facies and lacustrine facies in China, in China were still at the initial stage. Previous studies have focused on determining sedimentary environment, parent material type, organic matter abundance, and sedimentary model for shale of marine-continental transitional facies by the reservoir characteristics, gas bearing, Ro (%) and TOC (%) of shale (Guo and Wang, 2013; Qian et al., 2013; Wang et al., 2013; Sun et al., 2014; Guo et al., 2015; He et al., 2015; Li C. C. et al., 2015; Zhang et al., 2015; Liu et al., 2016; Su et al., 2016). At present, there is still a lack of systematic geochemical studies on marine-continental transitional facies shale. For example, the biomarker characteristics of marine-continental transitional facies shale are still unclear, What are the similarities and differences between its parent material source between marine-continental transitional facies and Marine shale? What is the hydrocarbon generating ability of marine-continental transitional facies shale?

So the study, for the first time, investigates the biomarker characteristics of marine-continental transitional facies shale, and compared those with the characteristics of shale for marine in China. The basic characteristics of marine-continental transitional facies shale were revealed from the Ebao area of the Qilian Basin in western China. Combined with the characteristics of basic geochemistry and petrology, this article discussed the source, keroger pattern, evolution degree and sedimentary environment, and evaluates the hydrocarbon generating ability of marine-continental transitional facies shale from the Ebao area of the Qilian Basin in western China. It provides reference for the research of marine-continental transitional facies shale in China and promotes the rapid development of marine-continental transitional facies shale gas. To achieve that, the shale in the in the southern Qilian Basin were analyzed by total organic carbon (TOC), Rock-Eval pyrolysis, biomarkers, and kerogen microscopy analyses.

Geological Setting

The studied sample were collected from ZK001 well and ZK2002 well, which is located in the southern Qilian Basin, China, which is one of the potentially key petroliferous basins. The southern Qilian Basin surrounded by the Qinghai Lake to the east, Hala Lake to the west, Zongwulong and South Qinghai Hills to the south, and mid-North Qilian Mountain to the north covers an NW-SE-oriented area of approximately 6.3×10^4 km^2. The southern Qilian Basin is composed of eleven first-order tectonic provinces, namely, the Tuoleinanshan uplift, the Shule depression, the Shulenanshan uplift, the Hala lake depression, the Baixingda uplift, the Muli depression, the Yangkang uplift, Xiariha depression, Tianpeng uplift, Tianjun depression and the Datongshan uplift.

The Muli depression is located in the north of Datong Mountain Uphold and adjacent to the north of Qilian Mountains and belong to the southern Qilian region, and extend NW-SE. It covers an area of about 2600 km^2. The sedimentary sequence within the Muli depression is well developed and preserved, and it contains Ordovician marine carbonate-detrital rocks, Silurian green and purple detrital rocks and slate, Permian marine carbonate and detrital rocks, Triassic carbonate and shale and sandstone. The Triassic strata are composed of the Huancang Formation (T_1x), Jianghe Formation (T_1j), Dajialian Formation (T_2d), Qieerma Formation (T_2q), Atasi Formation (T_3a), and Galedesi Formation (T_3g) (Fu and Zhou, 2000; **Figure 1**).

The ZK001and ZK2002 wells are located within the Muli depression and the target of the study is Galedesi Formation. The Galedesi Formation belongs to the marine-continental transitional sedimentary facies and is mainly composed of dark shale, sandstone, siltstone, and silty mudstone (Chen et al., 2016; **Figure 2**).

MATERIALS AND METHODS

Samples

A total of 31 samples were collected from ZK001 well and ZK2002 well in the southern Qilian Basin, China. The sample ZK001-1 to ZK001-20 are from ZK001 well, ranging in depth from 10.6 to 560.32 m. The lithologies are Mudstone, Gray Shale, Gray Mudstone, and Silty Shale. And the sample ZK2002-1 to ZK2002-11 are from ZK2002 well, ranging in depth from 158.00 to 1172.30 m. The lithologies are black shale, carbonaceous shale, coal, gray shale, and gray-black shale.

Organic Geochemical Experimental

The following organic geochemical experimental were carried out on 30 shales in the study area: TOC, rock pyrolysis, and the biomarkers by GC/MS (gas chromatography and mass spectrometry). The studied shales were crushed by a ball mill and ground to diameter less than 150 μm. About 50–100 mg shales were analyzed by means of a Rock-Eval 6 instrument made in France. The shales were pyrolysis by heating from 25 to 850°C at 10°C/min under a helium atmosphere, and then the pyrolytic indicators can be obtained, for example the TOC, volatile hydrocarbon (HC) (S_1), remaining HC generation potential (S_2), production parameter [$PI = S_1/(S_1 + S_2)$], hydrogen parameter ($HI = S_2/TOC \times 100$), and Tmax value (the temperature corresponding to the maximum value of S_2).

The Rock-Eval pyrolysis analyses were conducted using a Rock-Eval 6 instrument made in France. The Rock-Eval pyrolysis and TOC analyses were performed on 130 mg of ground material from the shale samples. The ground sample material was heated to 850°C at a rate of 10°C/min in a helium atmosphere.

Approximately 150 g of ground material from each shale sample was subjected to Soxhlet extraction using chloroform for 72 h at a constant temperature of 70°C. The extracts from the shale samples were deasphalted by precipitation with n-hexane and filtration. The deasphalted maltenes were fractionated into saturates and aromatics via column chromatography using

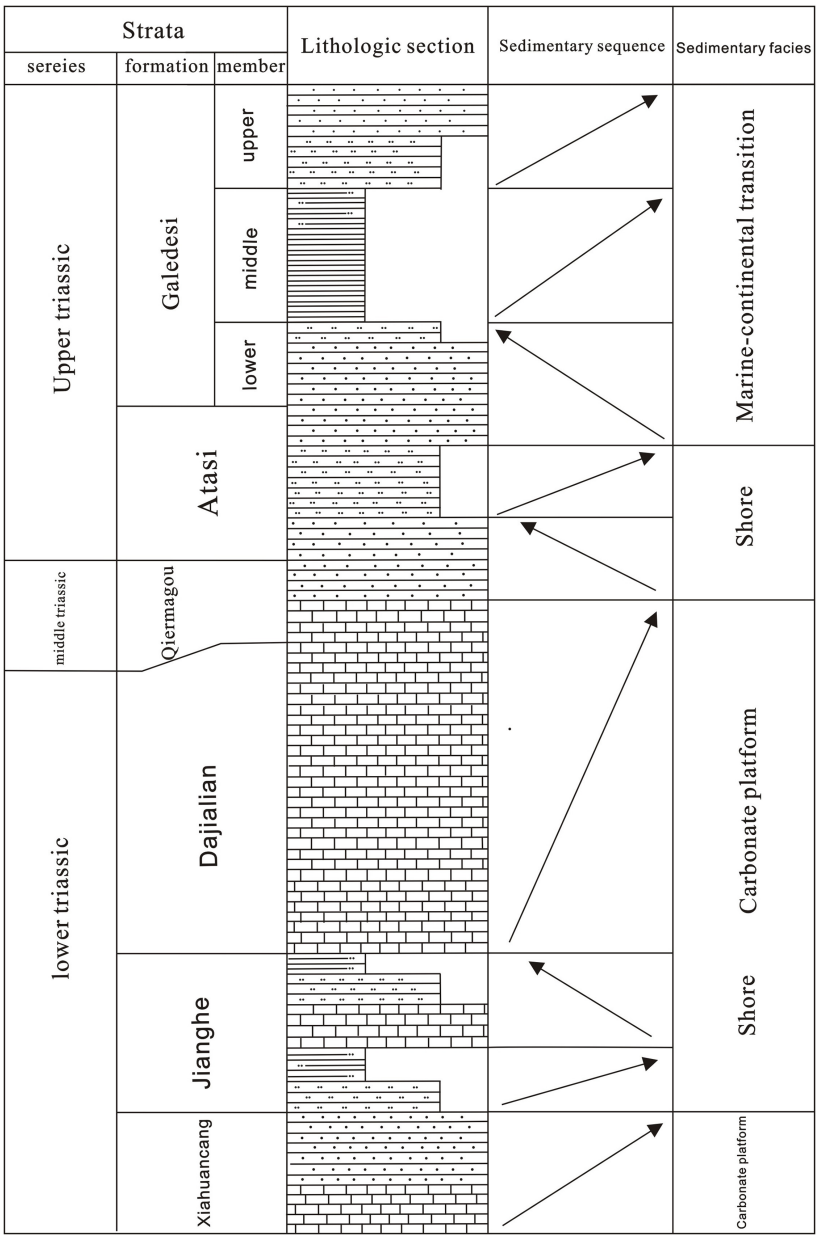

FIGURE 1 | Sedimentary facies of Triassic, Ebao area, Qilian Basin.

activated silica gel and aluminum oxide (*v: v* = 3:1) with n-hexane and methylene chloride, respectively (Wang et al., 2018). Saturates and aromatics were then analyzed by the GC-MS system. The GC-MS analyses were performed using an Agilent 6890N GC interfaced with a 5973 MS. An Agilent HP-5 column (30 m × 0.25 mm i.d., 0.25 μm film thickness) was used. The injection temperature was 70°C (2 min hold), and the temperature program was 4°C/min from 80 to 290°C (30 min hold). The flow rate of the carrier gas (He) was 1.1 mL/min, and the pressure was 2.4 kPa. The sample injection volume was 1.0 L, and the split ratio was 10:1. Electron impact (EI) ionization at 70 eV was used for the ion source. The temperatures of the transfer line and ion source were 280 and 230°C, respectively. The parent ion was m/z 285, the activating voltage was 1.5 V, and the scanning range was from m/z 35 to 600.

Petrographic Analyses

The vitrinite reflectance values were measured in random mode and reported in Ro (%). The samples were mounted in resin and were then ground into pellets and polished using alumina–ethanol slurry. The measurements were performed under oil immersion at a wavelength of 546 mm using a Leitz Orthoplan/MPV-SP photometer microscope system.

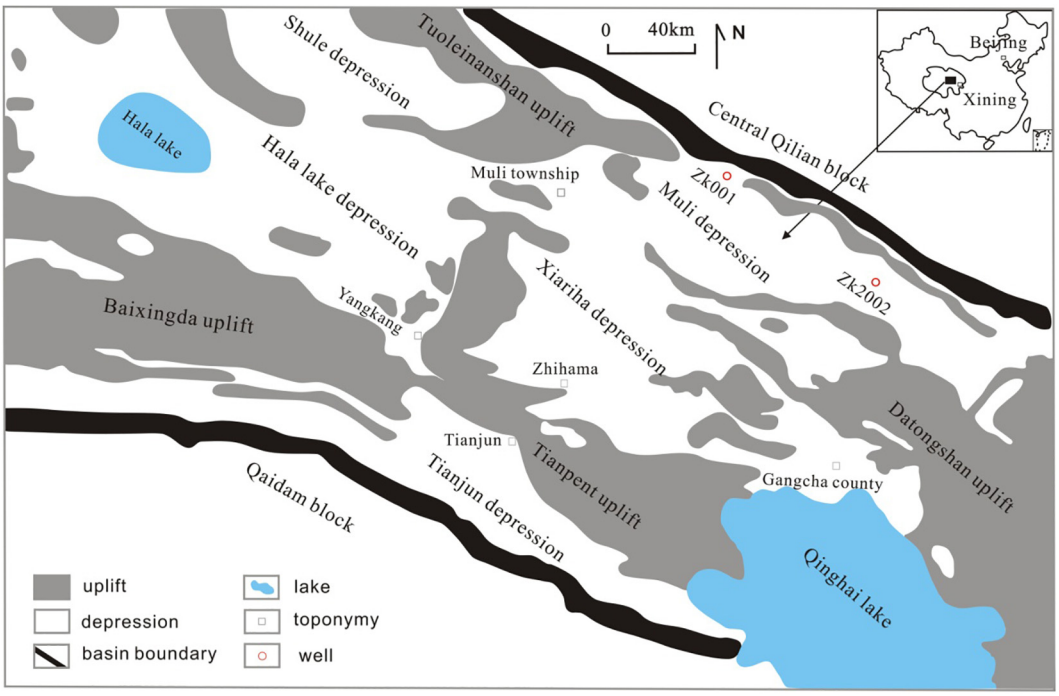

FIGURE 2 | Tectonic units in the Qilian Basin and the location of ZK001 well and ZK2002 well.

Petrographic analyses were performed on the polished shale samples under reflected white light following conventional methods using the Leitz Orthoplan/MPV-SP photometer microscope system. Each sample was measured at least 500 times.

RESULTS

TOC and Rock-Eval Pyrolysis

The TOC content and Rock-Eval data, including free hydrocarbons (S1), hydrocarbon generative potential (S2), temperature (Tmax) at the maximum of the S2 peak, and production parameter [PI = S1/(S1 + S2)], hydrogen parameter (HI = S2/TOC × 100), are listed in **Table 1**. The TOC of the 20 shale samples from ZK001well ranged from 0.85 to 3.73% (mean 1.45%), and the TOC of 10 shales from ZK2002 well ranged from 0.77 to 9.86% (mean 2.10%). The S1 values of the present shales from ZK001 well and ZK2002 well ranged from 0.01 to 0.32 mg HC/g and 0.01 to 0.08 mg HC/g, respectively. And the S2 values ranged from ZK001 well and ZK2002 well ranged from 0.06 to 4.20 and 0.02 to 1.24 mg HC/g, respectively. The Tmax values of the shale samples from ZK001 well and ZK2002 well ranged from 447 to 493 and 378 to 497°C, with an average value of 455 and 451°C, respectively. The HI values of the shale samples from ZK001well ranged from 6.63 to 154.54 mg HC/g TOC, with an average value of 33.16 mg HC/g TOC. And The HI values of the shale samples from ZK2002 well ranged from 3.18 to 54.52 mg HC/g TOC, with an average value of 19.97 mg HC/g TOC. The PI values of the shale samples from ZK001 well and ZK2002 well ranged from 0.07 to 0.26 and 0.03 to 0.21, with an average value of 0.14 and 0.10, respectively.

Vitrinite Reflectance and Maceral Groups

The vitrinite reflectance values (Ro, %) of the shale samples from ZK001 well and ZK2002 well ranged from 0.77–1.43 and 0.80–1.59%, respectively. The Ro values of 95% of the shale samples from ZK001 well fell within the range of 0.7–1.3%, and the Ro value of only one shale sample was greater than 1.3%. The Ro values of 60% of the shale samples from ZK2002 well fell within the range of 0.7–1.3%, and the Ro values of 40% of the shale samples fell within the range of 1.3–2.0% (**Figure 3**).

The shale samples from ZK001 well and ZK2002 well contain high vitrinite contents (mean content of 65.9 and 72.9%, respectively) and trace amounts of sapropelinite. Present samples from ZK001 well also contain abundant inertinite (5.0–47.1%) and small amounts of exinite (mean content of 1.21%). The most samples from ZK2002 well also contain abundant inertinite (3.0–47.2%) and small amounts of exinite (mean content of 0.28%). The kerogen type parameter (KTI) of the study samples well ranged from −85.45 to −75.00 and −96.25 to −75.75%, which were less than zero.

Molecular Composition of Hydrocarbons

Alkanes

The alkanes generally consist of *n*-alkanes and isoprenoid hydrocarbons. They were distributed differently in samples obtained from ZK001 well and ZK2002 well. The *n*-alkane distributions were unimodal in present samples from ZK001 well

TABLE 1 | Results of the Rock-Eval analyses performed on samples obtained from ZK001 well and ZK2002 well located in the Qilian Basin.

Sample	Well	Depth (m)	Lithology	TOC (*wt*%)	Rock-Eval pyrolysis				
					S1 (mg HC/g)	S2 (mg HC/g)	Tmax (°C)	HI (mg HC/g TOC)	PI
ZK001-1	ZK001	10.06	Mudstone	0.85	0.01	0.06	493	6.63	0.17
ZK001-2		70.32	Mudstone	1.48	0.09	0.63	447	42.65	0.12
ZK001-3		156.79	Gray shale	1.45	0.03	0.07	477	5.00	0.26
ZK001-4		185.75	Gray shale	1.90	0.21	0.93	453	49.16	0.19
ZK001-5		208.50	Gray shale	1.28	0.11	0.39	449	30.61	0.21
ZK001-6		223.30	Gray shale	1.39	0.09	0.44	453	31.67	0.16
ZK001-7		251.36	Gray shale	3.73	0.09	0.51	452	13.71	0.15
ZK001-8		322.10	Gray shale	1.21	0.08	0.38	454	31.04	0.18
ZK001-9		365.76	Gray shale	1.08	0.04	0.22	450	20.18	0.16
ZK001-10		377.75	Gray shale	1.34	0.09	0.52	452	39.25	0.14
ZK001-11		437.70	Gray shale	2.72	0.32	4.20	448	154.54	0.07
ZK001-12		449.87	Gray shale	1.72	0.18	0.88	455	51.22	0.17
ZK001-13		487.48	Gray shale	0.86	0.02	0.16	455	18.46	0.09
ZK001-14		504.21	Gray shale	0.85	0.03	0.14	461	16.02	0.17
ZK001-15		520.17	Gray shale	1.34	0.05	0.39	449	28.67	0.12
ZK001-16		544.97	Gray mudstone	1.05	0.02	0.25	455	23.49	0.09
ZK001-17		547.49	Silty shale	1.22	0.03	0.31	451	25.28	0.09
ZK001-18		555.90	Gray mudstone	1.24	0.03	0.24	452	19.16	0.10
ZK001-19		559.95	Gray shale	1.04	0.03	0.22	452	20.74	0.11
ZK001-20		560.32	Gray shale	1.28	0.04	0.46	448	35.67	0.09
ZK2002-1	ZK2002	158.00	Black shale	1.58	0.03	0.31	460	19.32	0.09
ZK2002-2		219.70	Carbonaceous shale	1.32	0.02	0.15	453	10.97	0.13
ZK2002-3		320.85	Carbonaceous shale	2.27	0.08	1.24	448	54.52	0.06
ZK2002-11		371.38	Coal	9.86	/	/	/	/	/
ZK2002-4		590.02	Gray shale	1.90	0.02	0.66	443	34.66	0.03
ZK2002-5		790.40	Gray shale	0.89	0.01	0.08	378	8.51	0.13
ZK2002-6		827.02	Carbonaceous shale	0.81	0.01	0.14	443	17.35	0.07
ZK2002-7		985.43	Carbonaceous shale	1.72	0.05	0.53	450	30.54	0.08
ZK2002-8		1108.00	Gray-black shale	1.02	0.01	0.11	454	10.82	0.10
ZK2002-9		1160.61	Gray-black shale	1.01	0.02	0.10	481	9.84	0.13
ZK2002-10		1172.30	Gray-black shale	0.77	0.01	0.02	497	3.18	0.21

HI = S2/TOC × 100 (mg HC/g TOC); PI = S1/(S1 + S2).

and ZK2002 well, and its maximum peak is the *n*-C_{16} (**Figure 4**, m/z 85). But the samples obtained from ZK001 well contained *n*-alkanes ranging from *n*-C_{13} to *n*-C_{32} [**Figure 4**, ZK001-8 (322.10 m)-m/z 85]. The *n*-alkane distribution pattern observed in the samples obtained from ZK2002 well reflected abundant *n*-C_{13} to *n*-C_{27} [**Figure 4**, ZK2002-4 (590.02 m)-m/z 85]. It was evident from **Figure 4**, m/z 85 that the relative abundance of high carbon *n*-alkanes (>C_{16}) from ZK001 well shales was higher than ZK2002 well shales.

The present samples from ZK001 well and ZK2002 well had carbon preference parameter (CPI) values that range from 0.98 to 1.32 and 1.02 to 1.69, respectively. The ΣnC/ΣnC ratios of the shale samples obtained from ZK001 well and ZK2002 well ranged from 1.15 to 2.81 and 2.31 to 30.84, respectively (**Table 2**).

Isoprenoid hydrocarbons were mainly by pristane (Pr) and phytane (Ph) (**Figure 3**). The Pr/Ph ratios of the samples obtained from ZK001 and ZK2002 well range from 1.52 to 2.43 and 1.49 to 2.40, respectively (**Table 2**), and are more than 1.0, indicating pristine dominance. The Pr/*n*-C_{17} and Ph/*n*-C_{18} values of the shale samples from ZK001 well were very low and ranged from 0.30 to 0.51 and 0.12 to 0.37, respectively (**Table 2**). And the Pr/*n*-C_{17} and Ph/*n*-C_{18} values of the shales from ZK2002 well were very low and ranged from 0.21 to 0.69 and 0.20 to 0.71, respectively (**Table 2**).

Tricyclic to Pentacyclic Terpanes

Tricyclic terpanes from C_{19} to C_{29} were present in the shale samples from ZK001 well and ZK2002 well, in which the content of C_{22} and C_{27} were very low (**Figure 4**, m/z 191). It showed an inverted "V" distribution with C_{23} the most prominent peak in the tricyclic terpanes series. The tricyclic terpanes C_{26} to C_{29} were the doublets contained S and R isomers, so they were doublets in the Ion chromatograms. Moreover, pentacyclic terpanes C_{27} to C_{35} were identified in the studied shale samples. Of these, C_{30}-αβ hopane was the highest relative abundance. The C_{27} trisnorhopane and homohopanes C_{31} to C_{35} appeared as doublets [18α (H) and 17α (H), 22S and 22R epimers, respectively] in the

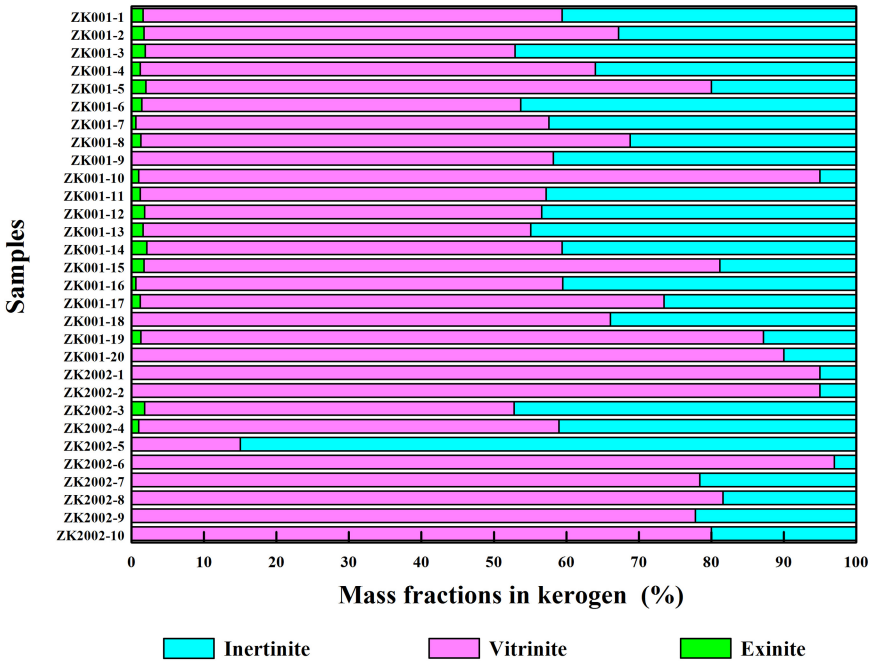

FIGURE 3 | Bar plot of maceral composition showing the mass fractions of inertinite, vitrinite, exinite, and sapropelinite for all shale samples obtained from ZK001 well and ZK2002 well in the Qilian Basin.

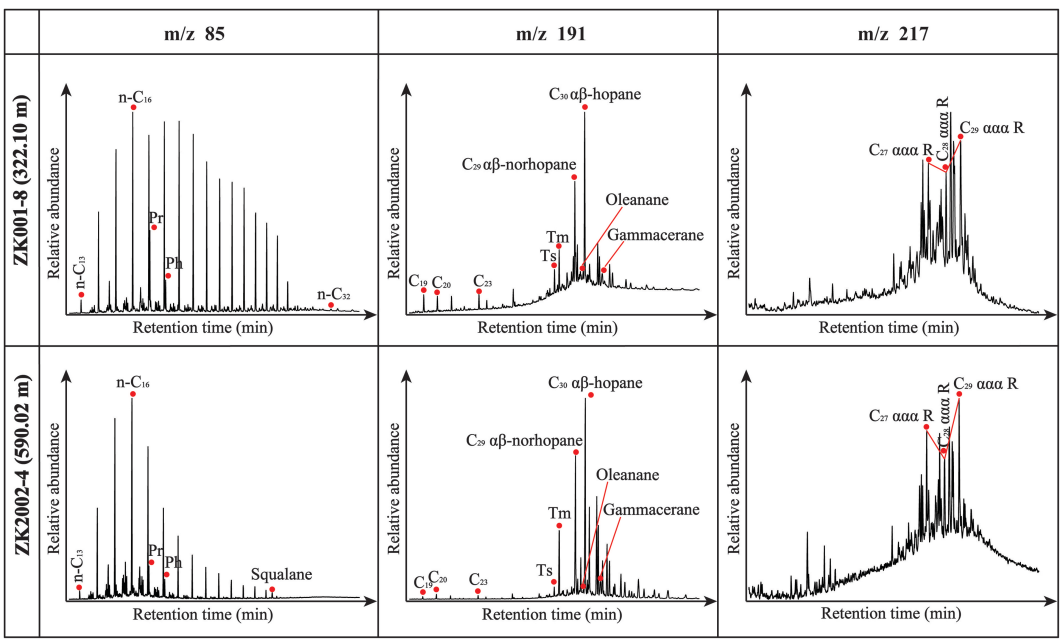

FIGURE 4 | Ion chromatograms of m/z 85 (*n*-alkanes and isoprenoid hydrocarbons), 191 (tricyclic to pentacyclic terpanes) and 217 (steranes) for saturate hydrocarbon (saturate hydrocarbon were separated from by column chromatography). With ZK001 well, ZK001-8 (322.10 m) is representative of all samples. With ZK2002 well, ZK2002-4 (590.02 m) is representative of all samples.

Ion chromatograms for all of the studied shales (**Figure 4**, m/z 191). Oleanane and gammacerane were also detected in in the shale samples from ZK001 well and ZK2002 well (**Figure 4**, m/z 191).

For present samples from ZK001 well, the maturity parameter $C_{31}22S/(22S + 22R)$ and Ts/Tm values of the pentacyclic terpane series ranged from 0.50 to 0.59 and 0.41 to 1.56, respectively (**Table 2**). And the maturity parameter $C_{31}22S/(22S + 22R)$ and

TABLE 2 | Molecular marker parameters and biomarker parameters for extracts from shale samples obtained from ZK001 well and ZK2002 well located in the Qilian Basin.

Sample	Pr/Ph	Pr/n-C_{17}	Ph/n-C_{18}	CPI	A	B	C_{27} (%)	C_{28} (%)	C_{29} (%)	C	D	E	F	G	H	DBT/P	MPI	Rc (%)	F (%)	DBF (%)	DBT (%)
ZK001-1	1.52	0.41	0.25	1.21	2.79	2.36	20.58	30.79	48.63	0.49	0.50	0.09	0.09	0.54	0.41	0.08	1.61	1.61	48.04	31.82	20.14
ZK001-2	1.67	0.43	0.37	1.11	2.81	2.21	21.35	31.56	47.09	0.48	0.53	0.11	0.14	0.52	0.47	0.11	0.94	1.21	45.61	30.99	23.40
ZK001-3	1.71	0.42	0.24	1.10	2.71	1.71	25.44	30.98	43.58	0.50	0.51	0.09	0.08	0.53	0.49	0.13	0.67	1.04	49.61	30.35	20.05
ZK001-4	1.81	0.47	0.25	1.10	2.61	1.53	27.31	31.03	41.66	0.55	0.51	0.13	0.15	0.59	1.56	0.08	0.80	1.12	41.99	35.08	22.93
ZK001-5	1.95	0.44	0.19	1.13	2.69	2.05	22.88	30.14	46.98	0.53	0.47	0.11	0.12	0.58	0.52	0.09	1.02	1.25	42.69	34.29	23.02
ZK001-6	1.91	0.40	0.18	1.02	2.73	2.36	21.12	29.08	49.80	0.49	0.49	0.09	0.08	0.56	0.54	0.11	0.67	1.04	43.07	36.75	20.18
ZK001-7	2.38	0.35	0.14	1.03	2.62	2.33	21.76	27.44	50.80	0.51	0.48	0.07	0.05	0.58	0.59	0.11	0.75	1.09	42.19	35.48	22.33
ZK001-8	2.43	0.47	0.17	0.99	2.63	1.21	31.99	29.22	38.79	0.50	0.44	0.08	0.06	0.58	0.59	0.10	0.76	1.10	51.68	31.73	16.59
ZK001-9	2.16	0.46	0.26	0.99	1.15	2.08	22.71	30.08	47.21	0.53	0.41	0.08	0.05	0.55	0.59	0.08	0.75	1.09	35.13	42.61	22.25
ZK001-10	2.01	0.41	0.29	0.98	1.29	2.15	22.29	29.68	48.03	0.47	0.42	0.10	0.10	0.54	0.61	0.07	0.96	1.22	44.80	35.89	19.31
ZK001-11	1.88	0.38	0.22	1.00	1.31	1.75	26.76	26.34	46.90	0.49	0.48	0.09	0.04	0.51	0.59	0.09	0.76	1.10	43.56	34.19	22.25
ZK001-12	1.89	0.39	0.20	1.23	1.21	1.79	26.54	25.87	47.59	0.49	0.50	0.11	0.07	0.52	0.61	0.08	0.91	1.18	41.29	38.56	20.15
ZK001-13	1.86	0.34	0.15	1.04	1.39	1.76	26.62	26.41	46.97	0.52	0.42	0.11	0.03	0.55	1.50	0.07	0.84	1.15	40.82	40.18	19.00
ZK001-14	1.71	0.35	0.19	1.00	1.33	1.74	27.40	24.98	47.62	0.51	0.50	0.10	0.04	0.52	0.61	0.06	0.84	1.14	41.50	33.21	25.30
ZK001-15	1.83	0.31	0.20	1.08	1.52	1.87	25.78	26.10	48.12	0.54	0.47	0.09	0.06	0.55	0.64	0.08	0.63	1.02	39.60	42.57	17.83
ZK001-16	2.07	0.30	0.12	1.02	1.74	1.98	23.50	30.07	46.43	0.49	0.47	0.06	0.02	0.57	0.56	0.08	0.98	1.23	41.56	31.55	26.89
ZK001-17	1.79	0.33	0.30	1.04	1.62	1.42	32.62	21.09	46.29	0.45	0.47	0.09	0.07	0.54	0.79	0.09	1.01	1.24	40.98	36.08	22.94
ZK001-18	1.85	0.50	0.25	1.32	1.54	1.94	24.29	28.56	47.15	0.53	0.48	0.09	0.04	0.52	0.85	0.09	0.64	1.03	42.69	35.21	22.10
ZK001-19	1.81	0.51	0.20	1.02	1.41	1.62	27.90	26.85	45.25	0.55	0.47	0.10	0.04	0.50	0.92	0.07	0.74	1.08	41.58	36.67	21.74
ZK001-20	2.11	0.50	0.21	1.01	1.51	2.03	23.01	30.36	46.63	0.55	0.42	0.11	0.02	0.59	1.00	0.09	0.63	1.02	40.97	36.54	22.49
ZK2002-1	1.87	0.35	0.71	1.69	30.84	1.16	34.99	23.69	40.68	0.44	0.42	0.16	0.06	0.55	0.82	0.27	0.70	1.06	50.55	3.72	45.74
ZK2002-2	1.91	0.40	0.66	1.20	3.01	1.40	31.03	25.41	43.56	0.47	0.44	0.15	0.06	0.52	0.85	0.21	1.08	1.29	40.58	29.85	29.57
ZK2002-3	2.14	0.46	0.49	1.04	2.67	1.22	34.72	23.09	42.19	0.43	0.42	0.16	0.03	0.53	0.85	0.19	0.86	1.16	39.59	30.29	30.12
ZK2002-4	2.40	0.69	0.49	1.02	2.50	3.83	16.70	19.30	64.00	0.44	0.36	0.16	0.02	0.58	0.14	0.12	0.74	1.08	16.72	68.04	15.24
ZK2002-5	2.30	0.51	0.46	1.13	2.74	1.34	34.21	19.99	45.80	0.43	0.44	0.13	0.03	0.57	0.85	0.09	1.20	1.36	46.59	28.62	24.79
ZK2002-6	1.83	0.50	0.35	1.26	2.60	1.50	31.35	21.56	47.09	0.49	0.50	0.15	0.04	0.52	0.85	0.10	1.01	1.25	45.86	29.87	24.27
ZK2002-7	1.71	0.21	0.20	1.11	16.10	1.48	31.32	22.18	46.50	0.45	0.46	0.13	0.05	0.59	0.82	0.06	0.86	1.16	39.06	45.45	15.49
ZK2002-8	1.63	0.52	0.37	1.09	2.31	1.53	30.23	23.65	46.12	0.48	0.46	0.14	0.04	0.54	0.89	0.08	0.90	1.18	47.59	27.85	24.56
ZK2002-9	1.59	0.57	0.49	1.18	2.69	1.68	28.02	24.98	47.00	0.42	0.45	0.14	0.05	0.51	0.89	0.09	0.92	1.19	48.59	24.98	26.43
ZK2002-10	1.49	0.50	0.65	1.17	18.66	1.13	35.29	24.97	39.74	0.41	0.41	0.14	0.05	0.60	0.89	0.07	0.70	1.06	43.20	39.53	17.27

Pr, pristane; Ph, phytane; CPI, carbon preference parameter; A, $\Sigma nC_{21}^{-}/\Sigma nC_{22}+$; B, C29/C27 regular steranes; C_{27}(%) = $C_{27}\alpha\alpha/C_{27}$–$C_{29}\alpha\alpha$ steranes; C_{28}(%) = $C_{28}\alpha\alpha/C_{27}$–$C_{29}\alpha\alpha$ steranes; C_{29} (%) = $C_{29}\alpha\alpha/C_{27}$–$C_{29}\alpha\alpha$ steranes; C, sterane $C_{29}\alpha\alpha$-20S/(20S + 20R); D, sterane C_{29}-ββ/(ββ + αα); E, gammacerane parameter, gammacerane/C_{30} αβhopane; F, oleanane parameter, oleanane/C_{30} αβhopane; G, hopane C_{31}-22S/(22S + 22R); H, Ts/Tm; Ts, 18α (H) -22, 29, 30-trinorhopane; Tm, 17α (H) -22, 29, 30-trinorhopane; DBT, dibenzothiophene; P, phenanthrene; MPI, methylphenanthrene parameter, MPI = 1.5(3-MP + 2-MP)/(P + 9-MP + I-MP); MP, methylphenanthrene; Rc, equivalent vitrinite reflectance (%); F, fluorine; DBF, dibenzofuran; F(%) = F/(F + DBF + DBT); DBF(%) = DBF/(F + DBF + DBT); DBT(%) = DBT/(F + DBF + DBT).

Ts/Tm values of the shales from ZK2002 well ranged from 0.51 to 0.61 and 0.14 to 0.89, respectively (**Table 2**).The gammacerane parameter (gammacerane/C_{30}-αβhopane) values of the present shales from ZK001 well and ZK2002 well range from 0.03 to 0.13 and 0.13 to 0.16 (**Table 2**), respectively. The oleanane parameter (oleanane/C_{30}-αβhopane) values of the shales from ZK001 well and ZK2002 well ranged from 0.02 to 0.15 and 0.02 to 0.06 (**Table 2**).

Steranes

The mass chromatograms of m/z 217of the present shales were mainly progesterones, rearrangement steranes, and regular steranes (**Figure 4**, m/z 217). The regular steranes were mainly the αα20S, ββ20R, ββ20S, and αα20R isomers, and ranged from C_{27} to C_{29} (**Figure 4**, m/z 217).

The ratios of C_{29} to C_{27} regular steranes (C_{29}/C_{27} regular steranes) of the shales from ZK001 well and ZK2002 well ranged from1.21 to 2.36 and 1.13 to 3.83, with an average value of 1.89 and 1.63, respectively. The maturity parameters of the steranes were C_{29}αα20S/(20S + 20R) and C_{29}ββ/(ββ + αα), and the values of these parameters of the shale samples from ZK001 well ranged from 0.45 to 0.55 and 0.41 to 0.53, respectively. For the shale samples from ZK2002, the values of C_{29}αα20S/(20S + 20R) and C_{29}ββ/(ββ + αα) ranged from 0.41 to 0.49 and 0.36 to 0.50, respectively. Additionally, the percentage of the regular steranes C_{27}αα20R, C_{28}αα20R and C_{29}αα20R of the shales from ZK001 well ranged from 20.58 to 32.62, 21.09 to 31.56, and 38.79 to 50.80%, respectively (**Table 2**), and the percentage of three steranes of shales from ZK2002 well ranged from 16.70 to 35.29, 19.30 to 25.41, and 39.74 to 64.00%, respectively (**Table 2**).

Aromatics

The aromatics from 2 to 5 aromatic rings were identified in the samples from ZK001 well and ZK2002 well (**Figure 5**). The major aromatics were naphthalene series compounds, phenanthrene series compounds, biphenyl series compounds, fluorene, dibenzofuran series compounds, dibenzothiophene, chrysene, fluoranthene and pyrene series compounds, perylene, and benzofluoranthene and benzopyrene.

The methylphenanthrene parameter (MPI), which is based on phenanthrene (m/z 178) and methylphenanthrenes (m/z 192) (**Figure 5**), was calculated as a maturation index (Radke, 1988). The MPI values of the present shales from ZK001 well range from 0.63 to 1.61 (**Table 2**). The equivalent vitrinite reflectance (Rc), which is based on an empirical relationship between the MPI and vitrinite reflectance, was used to assess maturity (Radke, 1988). The Rc values of the samples from ZK001 well range from 1.02 to 1.61% (**Table 2**). The MPI values of the shales from ZK2002 well range from 0.70 to 1.20, and the Rc (%) values range from 1.06 to 1.36% (**Table 2**).

The ratio of dibenzothiophene to phenanthrene (DBT/P) is believed to be an index of the Hydrocarbon forming paleoenvironment, the origin of parent materials and source rock lithology (Huang and Pearson, 1999). The DBT/P ratio from ZK001 and ZK2002 well shales ranged from 0.06 to 0.13 and 0.06 to 0.27, respectively (**Table 2**). With depth increasing the DBT/P values of samples from ZK001 well were decreased slowly, but the DBT/P values of shales from ZK2002 well ware decreased greatly.

Fluorene (F), dibenzothiophene (DBT), and dibenzofuran (DBF) are important aromatic compounds. They have been called three Fourene bacause of the similar chemical structure (Liu et al., 2013). The relative abundance of F, DBT, and DBF can indicate primary depositional environment of sedimentary organic matter, and can applied for oil-to-source and oil-to-oil correlation (Fang et al., 2016). The percentage of F, DBT, and DBF of the shales from ZK001 well ranged from 35.13 to 51.68, 16.59 to 26.89, and 30.35 to 42.61%, respectively (**Table 2**), and the percentage of F, DBT, and DBF of shales from ZK2002 well ranged from 16.72 to 50.55, 15.24 to 45.74, and 3.72 to 68.04%, respectively (**Table 2**).

DISCUSSION

Kerogen Microscopy Characteristics

The observation of kerogen indicates that the organic matter of the studies shale samples from ZK001 well and ZK2002 well was type III kerogen that included a moderate amount of inertinite, traces of sapropelinte, a high abundance of vitrinite and a low content of exinite (**Figure 3**). Type of kerogen can be used to the KTI, which is computed from the percentage composition of the kerogen components (Awan et al., 2020). The KTI values of the studied shales from ZK001 well and ZK2002 well were less than zero, reflecting type III kerogen (Awan et al., 2020).

Total Organic Carbon and Types of Organic Matter

Total organic carbon (*wt*%) was used to evaluate the abundance of organic matter and the hydrocarbon generation potential of the samples (Gonzaleza et al., 2020). A total of 85% of the samples from ZK001 well can be deemed as "good to very good" source rock quality (> 1.0%), and 15% of the samples classified as "fair" source rock quality (0.5–1.0%) (**Figure 6**). For ZK2002 well, 70% of the samples can be belonged to "good to very good" source rock quality (> 1.0%), and 30% of the samples classified as "fair" source rock quality (0.5–1.0%) (**Figure 6**).

The studied shales from ZK001 well and ZK2002 well had low the hydrogen index (HI) (**Table 1**). The relationship between HI and Tmax indicates the organic matter of the studied shales was predominantly type III (Hu et al., 2018; **Figure 7**). A plot of TOC and S_2 is also used to indicate the kerogen type of source rack (Tao et al., 2013). The relationship between TOC and S_2 indicates the organic matter of type III in the studied shale from ZK001 well ZK2002 well (**Figure 8**).

Sources of the Hydrocarbons

The percentage composition of C_{27}–C_{29} αα 20R steranes can be used to indicate differences in the origins of organic matter, because C_{29} sterane may have contributed to the terrigenous materials (especially higher plants), C_{28} sterane may have derived from the lower land plants (lichens and mosses), and C_{27} sterane may have originated from the zooplankton

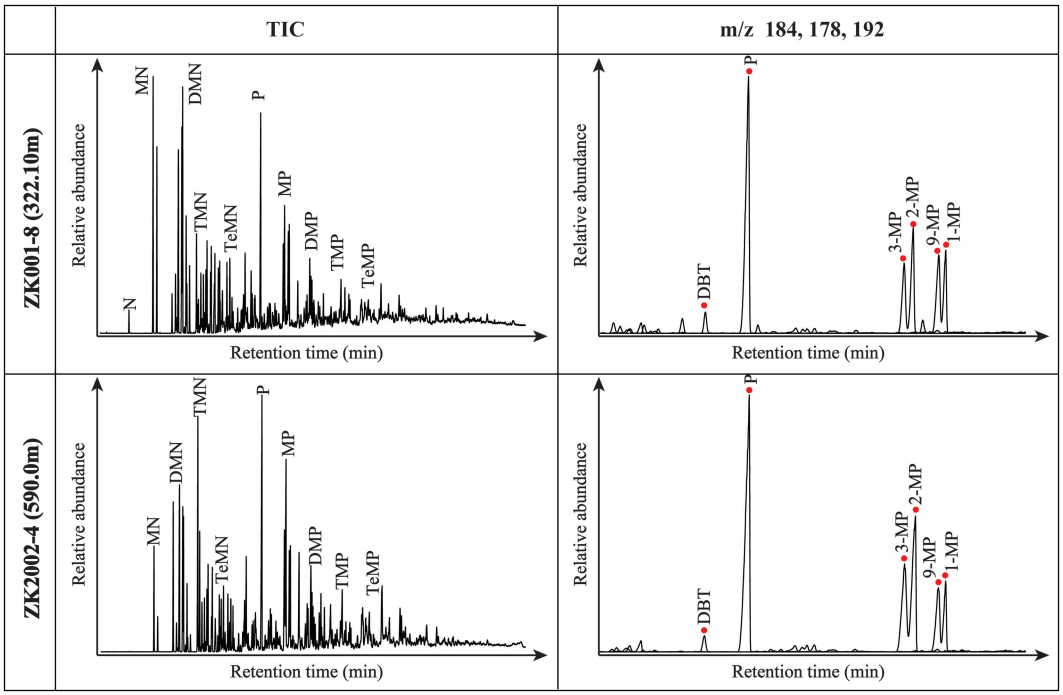

FIGURE 5 | Gas chromatograms (TIC) and ion chromatograms of m/z 184 (dibenzothiophene), 178 (phenanthrene), and 192 (methylphenanthrenes) for aromatics of extracts from the present samples. With ZK001 well, the ZK001-8 (322.10 m) is representative of all samples. With ZK2002 well, the ZK2002-4 (590.02 m) is representative of all samples.

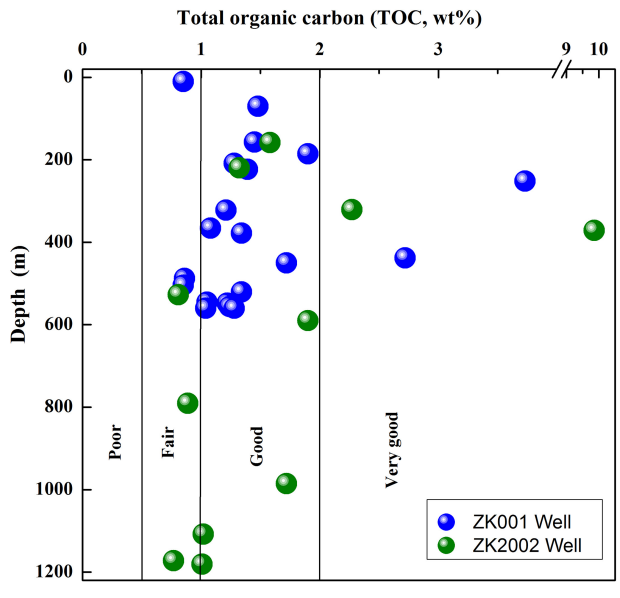

FIGURE 6 | Distribution of total organic carbon (TOC, *wt*%) versus depth (m) for the shale samples obtained from ZK001 well and ZK2002 well.

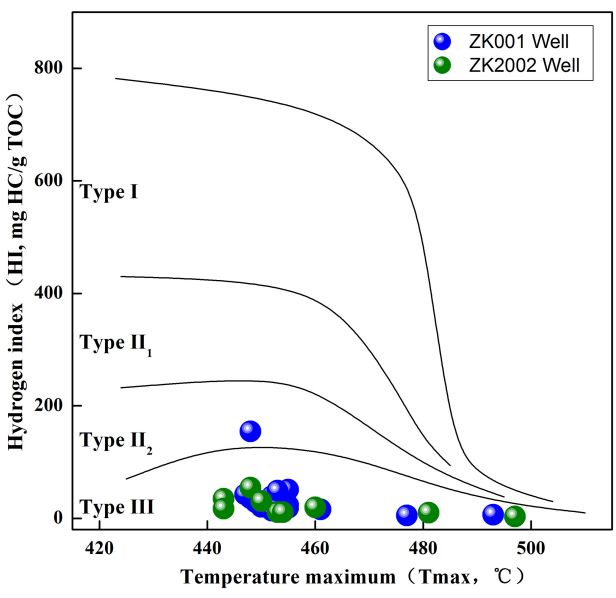

FIGURE 7 | Plot of hydrogen parameter (HI) versus Tmax and showing the kerogen types of the shale samples obtained from ZK001 well and ZK2002 well.

(El-Sabagh et al., 2020). The percentage composition of C_{27} ααα 20R sterane in the samples from ZK001 well and ZK2002 well were similar to or slightly lower than the percentage composition of C_{29} αα 20R steranes (**Figure 9**), indicating that the organic matter of the studied shales have originated from a mix of zooplankton and terrestrial organic sources (El-Sabagh et al., 2020). The relationship between Pr/*n*-C_{17} and Ph/*n*-C_{18} ratios

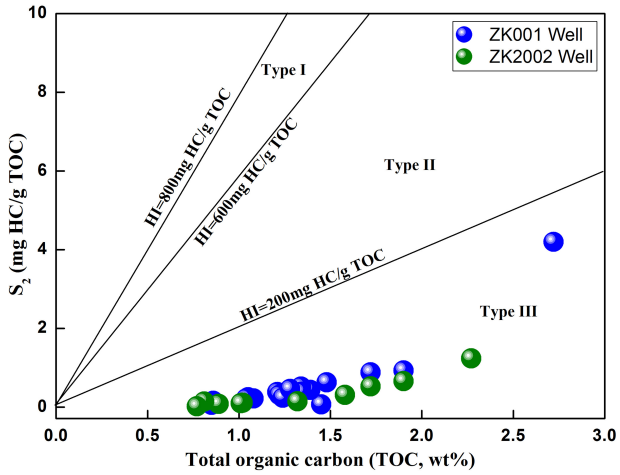

FIGURE 8 | Plot of TOC *wt*% versus S_2 mg HC/g TOC showing the kerogen types of the shale samples obtained from ZK001 well and ZK2002 well.

can be used to determine the Sources of the hydrocarbons (El-Sabagh et al., 2020). A plot of the Pr/*n*-C_{17} and Ph/*n*-C_{18} ratios (**Figure 10**) shows that the shales from ZK001 well and ZK2002 well were derived from a mixed organic matter, but the terrigenous organic matter of the shales from ZK001 well may be greater than the shales from ZK2002 well.

Depositional Environments

Many indicators of biomarkers can be indicated the depositional environment of the organic matters, such as pristane/phytane (Pr/Ph), Pr/*n*-C_{17}, Ph/*n*-C_{18}, the relationship between C_{27}, C_{28}, and C_{29} αα steranes, gammacerane and oleanane, and the relative abundance of F, DBT, and DBF.

The percentage composition of C_{27}, C_{28}, and C_{29} αα 20R steranes can be used to evaluate the hydrocarbon generation environments (El-Sabagh et al., 2020). The studied shale samples from ZK001 well and ZK2002 well plotted in the estuarine/bay portion of the ternary diagram (**Figure 9**).

The Pr/Ph ratio generally indicated the redox degree of the hydrocarbon generation environments and varied with water depth. High Pr/Ph values reflect oxidation environments, shallow water and terrestrial inputs (El-Sabagh et al., 2020). The Pr/Ph values of the shales found at depths of 10.06–322.10 m in ZK001 well tended to increase with increasing shale depth (**Figure 11**). By contrast, the Pr/Ph values in samples found at depths of 322.10–560.32 m tended to decrease with increasing shale depth (**Figure 11**). In the meantime, the Pr/Ph values of the shales found at depths of 158.00–590.02 m in ZK2002 well tended to increase with increasing shale depth and the Pr/Ph values in shales found at depths of 590.02–1172.30 m tended to decrease with increasing shale depth (**Figure 11**). Therefore, the hydrocarbon generation environments of the shales from ZK001 well and ZK2002 well transitioned from deep to shallow to deep, which is typical of sediments found in marine-continental transitional sedimentary facies. The relationship between Pr/*n*-C_{17} and Ph/*n*-C_{18} in the shale samples from ZK001 well ZK2002 well supported this interpretation and indicated a oxidizing to weakly reducing pattern characteristic of sediments deposited in alternating sea and riverine facies (**Figure 10**; El-Sabagh et al., 2020).

Gammacerane is an important biomarker and may derive from tetrahymanols, which are existed in marine sediments (El-Sabagh et al., 2020; Martins et al., 2020). High gammacerane contents are typical of high-salinity environments and commonly result from hypersalinity and suboxidation at depth (Sousaa et al., 2019). Therefore, the abundance of gammacerane can be used to recognize the existence of stratified water columns in the hydrocarbon generation environments of marine and non-marine organic matter (Holba et al., 2003). The studied shales of ZK001 well and ZK2002 well had low the gammacerane parameter (gammacerane/C_{30}-αβ hopane) values. This range indicated weakly reducing, brackish conditions during the deposition of the shales (El-Sabagh et al., 2020), and the degree of reducing environment and brackish conditions of the shales from ZK001 well might be less than the shales from ZK2002 well. The ratio of dibenzothiophene to phenanthrene (DBT/P) was also a good indicator the hydrocarbon generation environments, organic matter origin and the main lithology (Huang and Pearson, 1999). A plot of the DBT/P and Pr/Ph ratios (**Figure 12**) shows that the studied shales from ZK001 well and ZK2002 well fell on the boundary between marine and lacustrine shale.

Oleanane, an important biomarker of terrigenous materials, has been indicated as an index of angiosperms (flowering plants) (El-Sabagh et al., 2020). The ratio of oleanane to C_{30}-αβ hopane (the oleanane parameter) provided information about the hydrocarbon generation environments and source rock ages (El Diasty et al., 2020). Oleanane index value less than 0.2 to show that the sample was deposited during marine deltaic or marine shelf environments (Cortes et al., 2013). By contrast, oleanane index values more than 0.2 are characteristic of the tertiary and in a marine deltaic environment (Cortes et al., 2013). **Figure 8** can be used to evaluate the depositional environment of oils and source rocks based on the relationship between Pr/Ph and oleanane parameter. The **Figure 13** indicates that the shales from ZK001 well and ZK2002 well are likely associated with a marine shelf to deltaic depositional environment, but the depositional environment of the most of the studied shales were marine shelf environment.

The triangular diagram of the proportion of Fs, DBFs, and DBTs in aromatic compounds can indicate primary depositional environment of sedimentary organic matter (Fang et al., 2016). **Figure14** shows the percentage content of three fluorenes of the studied shales from ZK001 well and ZK2002 well using a triangular diagram. The shales from ZK001 well and ZK2002 well are characterized by low percentage content of DBTs, with the ratio of DBTs/(Fs + DBFs + DBTs) < 30% (**Table 2**), inferring a oxidizing to weakly reducing depositional environment and a marine and lacustrine shales.

Maturity

Many geochemistry indexes can be indicated the evolution degree of the organic matters, such as Ro, Tmax, CPI, the correlation of Pr/*n*-C_{17} and Ph/*n*-C_{18}, sterane C_{29}αα20S/(20S + 20R) and

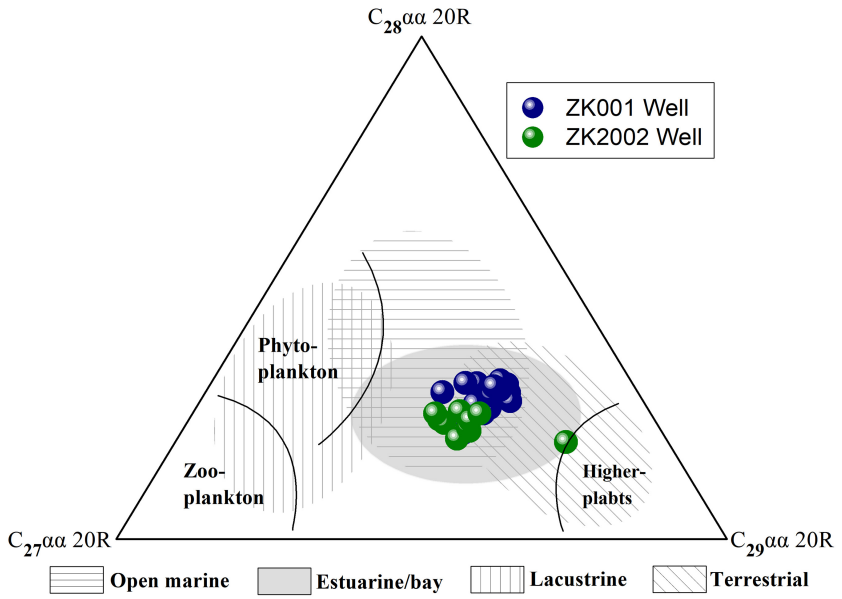

FIGURE 9 | Ternary plot showing the relative contents of C_{27}–C_{29} αα 20Rsteranes for shale samples obtained from ZK001 well and ZK2002 well.

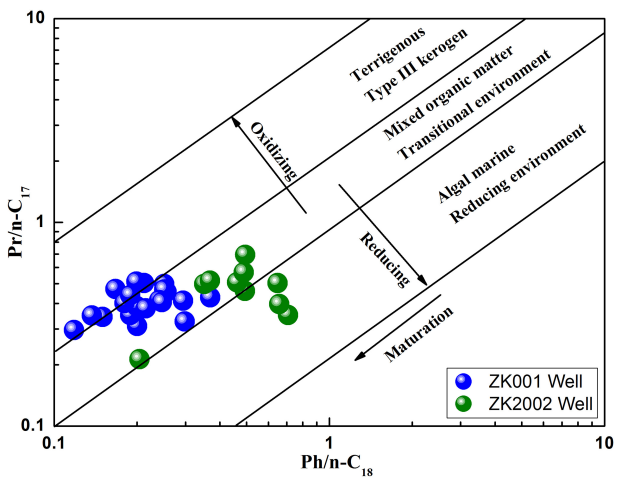

FIGURE 10 | Plot of Pr/*n*-C_{17} versus Ph/*n*-C_{18} for shale samples obtained from ZK001 well and ZK2002 well.

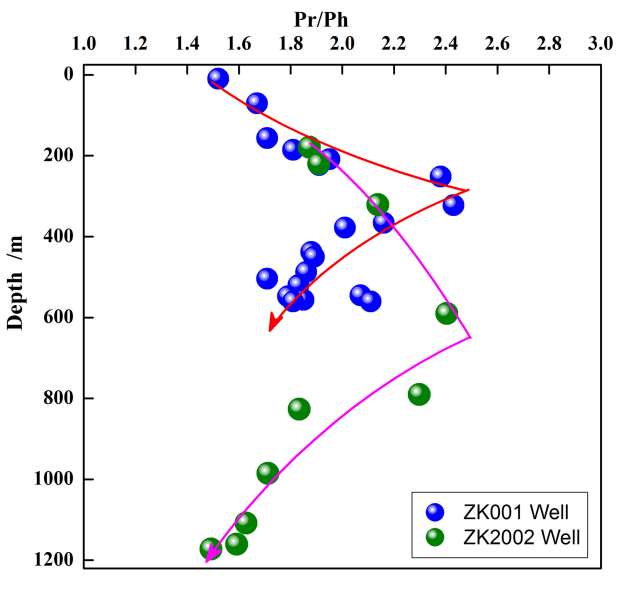

FIGURE 11 | Ratio of Pr/Ph with depth of the shale from ZK001 well and ZK2002 well.

C_{29}ββ/(ββ + αα), hopane C_{31}ααα22S/(22S + 22R) and Ts/Tm, the MPI and the equivalent vitrinite reflectance (Rc).

The Ro (%) values of the shales from ZK001 well and ZK2002 well were greater than 0.7%, showing a high degree of maturity. According to the Ro (%) values, 95% of the shales from ZK001 well and 60% of the shales from ZK2002 well can be considered as mature (0.7–1.3%), and 10% shales from ZK001 well and 40% of the shales from ZK2002 well can be thought of as highly mature (1.3–2.0%) (Radke, 1988).

The Tmax values of the shales from ZK001 well and ZK2002 well (except for ZK2002-5) were greater than 440°C (**Table 1**), showing maturity to highly mature (Tao et al., 2013).

The CPI values of the n-alkanes, the correlation of Pr/*n*-C_{17} and Ph/*n*-C_{18}, the sterane C_{29}αα20S/(20S + 20R) and C_{29}ββ/(ββ + αα), the hopane C_{31}ααα22S/(22S + 22R) and Ts/Tm (Fang et al., 2019), the MPI and the equivalent vitrinite reflectance (Rc) (Radke, 1988) are considered effective maturity indicators.

For the studied most of the shales, the CPI values were close to 1.0 (**Table 2**) and indicative of the mature stage (Li et al., 2017). As may be seen from the **Figure 10**, the organic matters of the

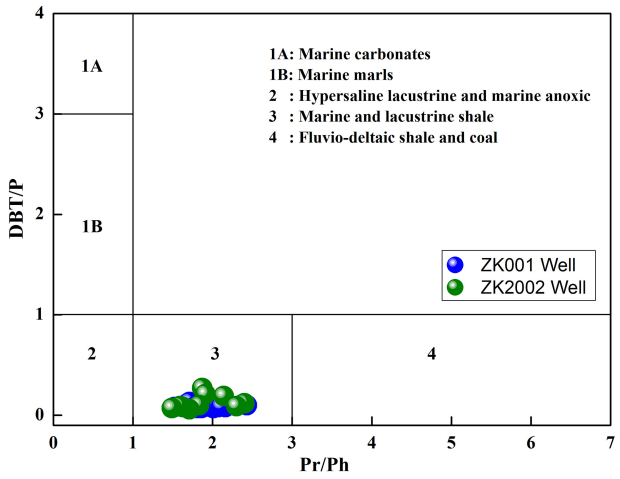

FIGURE 12 | Ratio of dibenzothiophene to phenanthrene (DBT/P) plotted against the ratios of Pr/Ph to determine shale depositional environments from ZK001 well and ZK2002 well.

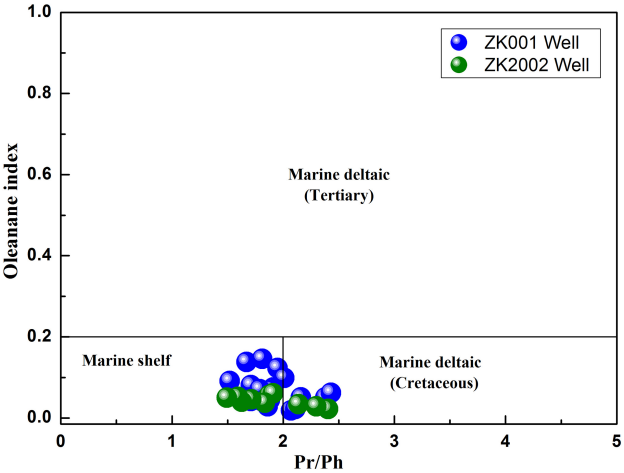

FIGURE 13 | Plot of oleanane parameter values versus the Pr/Ph ratio, indicating the depositional environment of the shale from ZK001 well and ZK2002 well.

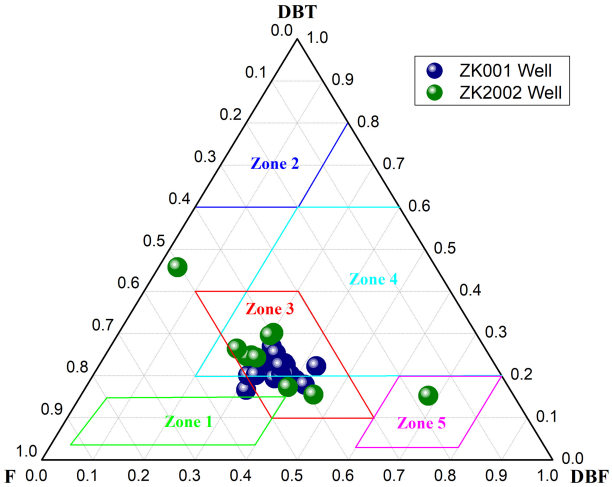

Zone 1:Fluvial/deltaic/fresh water lacustrine shale. **Zone 2**:Marine carbonate. **Zone 3**:Marine shale. **Zone 4**:Brackish/saline lacustrine shale. **Zone 5**:Swamp.

FIGURE 14 | Triangular diagram of the proportion of three fluorenes in aromatic compounds of the shale from ZK001 well and ZK2002 well.

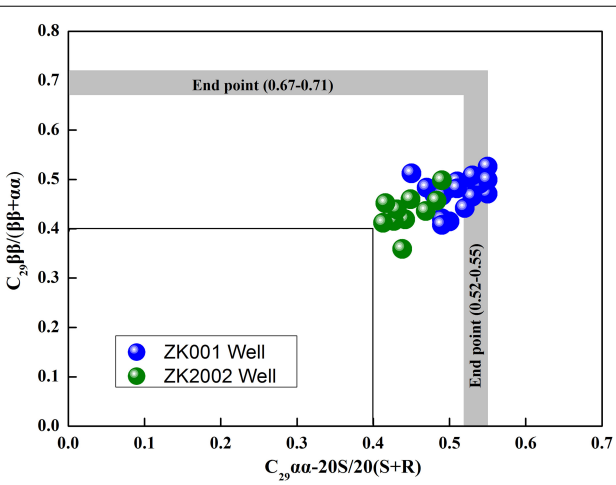

FIGURE 15 | Plot of the sterane parameter $C_{29}\beta\beta/(\beta\beta + \alpha\alpha)$ versus the sterane parameter $C_{29}\alpha\alpha 20S/(20S + 20R)$, indicating the maturity of the shale samples obtained from the shales from ZK001 well and ZK2002 well.

studied shales from ZK001 well and ZK2002 well were in the high maturity stage, and the maturity of the shales from ZK001 well was higher than the maturity of the shales from ZK2002 well (El-Sabagh et al., 2020).

Most of the studied shales yielded high values of the sterane parameter $C_{29}\beta\beta/(\beta\beta + \alpha\alpha)$, except for sample ZK2002-4. The equilibrium values of sterane parameter [$C_{29}\alpha\alpha 20S/(20S + 20R)$ and $C_{29}\beta\beta/(\beta\beta + \alpha\alpha)$] is 0.52–0.55 and 0.67–0.71, respectively (Chen et al., 2016). It is generally believed that when the sterane parameters is greater than 0.40, the sample has characteristics of mature organic matter (Chen et al., 2016). The sterane parameters of shales from ZK001 well and ZK2002 well indicate that the organic matter in the samples is mature to high mature [$C_{29}\beta\beta/(\beta\beta + \alpha\alpha)$ of the most shales from ZK001 well had been to the equilibrium value], and the maturity of the shales from ZK001 well were higher than the shales of ZK2002 well (**Figure 15**).

A maturity of the organic matter can also evaluated by means of the values of the hopane parameter $C_{31}22S/(22S + 22R)$ and Ts/Tm (Chen et al., 2016). The hopane parameters indicate that the samples obtained from ZK001 well and ZK2002 well were mature (**Table 2**).

The MPI and the equivalent vitrinite reflectance (Rc, %) can also mean to be maturity parameter (Radke, 1988). The MPI and Rc values (**Table 2**) indicated that the studied shales from ZK001 well and ZK2002 well were mature.

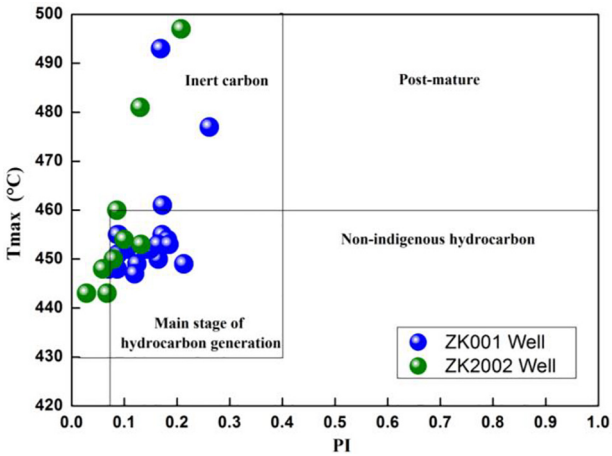

FIGURE 16 | Plot of pyrolysis-based Tmax versus production parameter (PI) values reflecting the degree of maturation and nature of the hydrocarbon products in the shale samples obtained from ZK001 well and ZK2002 well in China.

Hydrocarbon-Generating Potential

The gas potential of shale could be inferred for several standard methods. Zou et al. (2010) and Zumberge et al. (2012) considered that shale should be in accordance with some geochemical standard be kinked a high shale gas potential (Zou et al., 2010; Zumberge et al., 2012). For example, the TOC may be more than 2.0%, the Ro would be greater than 0.8–1.1%, and the kerogen ought to be type II or III. Moreover, Nie et al. (2009) and Li et al. (2011) suggested that the high maturity shales with TOC greater than 1.0% for China can be considered to have great hydrocarbon generation potential (Nie et al., 2009; Li et al., 2011). For the shales from ZK001 well and ZK2002 well, the TOC contents of 85 and 70% of the samples were greater than the 1% threshold value (average TOC content: 1.45 and 1.33%), respectively. All of the shales from ZK001 well and ZK2002 well were at a maturity to high maturity level that is competent to generate shale gas. The indicators of depositional environment and kerogen type indicated a marine shelf depositional environment and type III organic matter for all of shales. Therefore, our data and interpretations, namely the relatively high TOC contents and high maturities and type III organic matter of the organic matter in ZK001 well and ZK2002 well showed that the studied shales were appropriate for commercial shale gas production.

Besides, the Tmax and PI values from the Rock-Eval pyrolysis analyses are used to evaluate the hydrocarbon generation potential and the degree of maturation for source rock (Hakimi and Abdullah, 2013). The relationship between Tmax and PI showed that the most of shales from ZK001 well and ZK2002 well are in the main stage of hydrocarbon generation (**Figure 16**).

TABLE 3 | Relevant parameters of marine-continental transitional facies shale in the Qilian Basin and comparison with important shale in major basins or regions.

Sedimentation type	Basin or region	Layer	TOC/%	Type	Ro/%	Data sources
Marine	Sichuan Basin Southern China	Jiusi Formation	0.61–15.90	I–II	1.34–2.22	Dai et al., 2020
		Wufeng-Longmaxi Formation	0.41–25.73	I–II	1.60–4.91	Dai et al., 2020
		Qiongzhusi Formation	0.35–22.15	I	1.28–5.20	Dai et al., 2020
		Doushantuozu Formation	0.58–12.00	I	2.00–4.50	Dai et al., 2020
		Longmaxi Formation	0.81–7.28	I–II	/	Tuo et al., 2016
		Longmaxi Formation	1.13–4.43	I–II	1.59–2.62	Ma et al., 2012
		Niutitangzu Formation	0.29–15.69	$I–II_1$	2.30–3.19	Guo et al., 2019
Marine-continental transitional facies	Qilian Basin	Galedesi Formation	0.77–9.86	III	0.77–2.00	This study
	Qaidam Basin	Carboniferous	0.29–14.10	III	1.09–1.53	Wang et al., 2018
	Sichuan Basin	Liangshan-Long Formation	0.50–12.55	III	1.80–3.00	Dai et al., 2020
	East Yunnan-Western Hubei	Long Formation	0.35–6.50	III	2.00–3.00	Dai et al., 2020
	Middle-lower Yangtze	Long Formation	0.10–12.00	III	1.30–3.00	Dai et al., 2020
	South China	Long Formation	0.10–10.00	III	2.00–4.00	Dai et al., 2020
	Ordos Basin	Shanxi Formation	0.50–31.00	III	0.60–3.00	Dai et al., 2020
		Taiyuan Formation	0.50–36.79	III	0.60–3.00	Dai et al., 2020
		Benxi Formation	0.50–25.00	III	0.60–3.00	Dai et al., 2020
	Bohai Bay Basin	Permian	0.50–3.00	III	0.50–2.60	Dai et al., 2020
		Carboniferous	0.50–3.00	III	0.50–2.80	Dai et al., 2020
Continental	Songliao Basin	Third member Shahejie	0.50–13.80	$I–II_1$	0.40–2.00	Dai et al., 2020
		Fouth member Shahejie	0.80–16.70	II_1	0.60–3.00	Dai et al., 2020
	Bohai Bay Basin	Xujiahe Formation	1.00–4.00	$III+II_2$	1.60–3.60	Dai et al., 2020
Marine	Louisiana	Wolfcamp	4.0–9.8	$I–II_1$	1.2–4.5	Dai et al., 2020
	/	Fayetteville	1.0–14.0	$I–II_1$	1.1–3.0	Dai et al., 2020
	Anadarko	Woodford	2.0–6.0	$I–II_1$	1.1–2.1	Dai et al., 2020
	Michigan	Barnett	0.7–6.2	II_1	2.2–3.2	Dai et al., 2020

TABLE 4 | Relevant biomarker parameters of marine-continental transitional facies shale in the Qilian Basin and comparison with important shale in major basins or regions.

Sedimentation type	Basin/region	Layer	Pr/Ph	OEPCPI	Distribution of sterane	Sterane C_{29}-20S/(20S + 20R)	Sterane C_{29}-ββ/(ββ + αα)	Hopane C_{31}-22S/(22S + 22R)	Hopane Ts/Tm	Data sources
Marine-continental transitional facies	Qilian Basin	Galedesi Formation	1.91	0.981.11	$C_{29} > C_{27} > C_{28}$	0.49	0.46	0.55	0.74	This study
	Qaidam Basin	Carboniferous	1.17	0.931.04	$C_{29} > C_{27} > C_{28}$	0.44	0.46	0.59	1.04	Wang et al., 2018
Marine facies	Sichuan Basin	Longmaxi Formation	0.76	//	$C_{27} > C_{29} > C_{28}$	0.42	0.36	0.64	0.73	Tuo et al., 2016
			0.551	1.081.28	$C_{27} > \approx C_{29} > C_{28}$	0.43	/	0.52	/	Ma et al., 2012
	Northwest Hunan	Niutitangzu Formation	0.31	//	$C_{27} > C_{29} > C_{28}$	0.46	0.62	0.60	0.56	Guo et al., 2019
	Nayong area, western Guizhou	Niutitangzu Formation	0.29	1.08/	$C_{27} > C_{29} > C_{28}$	0.39	0.41	0.59	0.75	Wang et al., 2011
Continental facies	Ordos Basin	Yanchang Formation	1.37	1.021.08	$C_{29} > \approx C_{27} > C_{28}$	0.49	0.62	0.52	4.57	Zhang et al., 2013
	Sichuan Basin	Xujiahe Formation/Zilijing Formation	1.21	1.071.04	$C_{29} > C_{27} > C_{28}$	0.42	0.38	0.60	0.78	Huang et al., 2020

Therefore, the geochemical characteristics showed that the shales from ZK001 well and ZK2002 well have very good gas generation potential.

Comparison of Geochemical Characteristics of Shale

From the point of view of TOC, the abundance of organic matter of shale is high (average > 1.6%) (**Table 3**) in marine-continental transitional facies shale from Qilian Basin and shale of marine, continental and marine-continental transitional facies in China and the major regions of the United States (for example, Barnett, Haynesville, and Woodford) (Ma et al., 2012; Tuo et al., 2016; Wang et al., 2018; Dai et al., 2020). The minimum TOC of marine-continental transitional facie shale in Qilian Basin was higher than marine-continental transitional facie shale in other regions of China (**Table 3**), which indicates that the percentage of high-quality shale in the Qilian Basin shale is higher.

From maturity, the shales of marine and marine-continental transitional facies shale in Sichuan Basin and South China, from maturity, were in the high-over mature stage (**Table 3**; Ma et al., 2012; Tuo et al., 2016; Wang et al., 2018; Dai et al., 2020). Similarly, the shales in the major regions of the United States (for example, Barnett, Haynesville, and Woodford) were also in the high-over mature stage (Dai et al., 2020). And the marine-continental transitional facies shale from Qilian Basin, Ordos Basin, Bohai Bay Basin, Qaidam Basin and the continental shale in China had from the mature to over mature stage (**Table 3**).

The type of organic matter for marine-continental transitional facies shale in Qilian Basin and Major regions of China were all Type III (**Table 3**), which were quite different from the marine and continental shale in China and the shale in the major areas of the United States (such as Barnett, Haynesville, Woodford) (Ma et al., 2012; Tuo et al., 2016; Wang et al., 2018; Dai et al., 2020).

In terms of biomarkers of shale, the marine-continental transitional facies shale in Qilian Basin and the marine-continental transitional facies shale in Qilian Basi and the marine shales and the continental shales in China were in the mature stage (Wang et al., 2011, 2018; Ma et al., 2012; Zhang et al., 2013; Tuo et al., 2016; Guo et al., 2019; Huang et al., 2020). This conclusion could be enables by various geochemical parameters, such as OEP and CPI and Sterane C_{29}-20S/(20S + 20R) and Sterane C_{29}-ββ/(ββ + αα), and hopane C_{31}-22S/(22S + 22R) and hopane Ts/Tm (**Table 4**).

The difference were that the origin of organic matter input for marine-continental transitional facies shales in Qilian Basin and Qaidam Basin was mainly humic in a oxidizing to weakly reducing pattern characteristic of sediments deposited (**Table 4**). The hydrocarbon generation environments of the shale transitioned from deep to shallow to deep. However, the parent material of marine shale in Sichuan Basin and South China is mainly derived from aquatic organisms, and its hydrocarbon-forming environment was the strong-reduced marine sedimentary environment (**Table 4**). The parent material of continental shale in Sichuan Basin and Ordos Basin is mainly derived from terrigenous organic matter, and its hydrocarbon-forming environment was the shallow-water

sedimentary environment (**Table 4**; Wang et al., 2011, 2018; Ma et al., 2012; Zhang et al., 2013; Tuo et al., 2016; Guo et al., 2019; Huang et al., 2020). This conclusion could be enables by the geochemical parameters Pr/Ph and the distribution characteristic of sterane.

Based on the geochemical characteristics of organic matter abundance, organic matter type, parent material source and maturity of marine-continental transitional facies shale in Qilian Basin, the marine-continental transitional facies in Qilian Basin had the same high quality shale as the marine and continental shale in China. This implies that the marine-continental transitional facies shale in Qilian Basin had a good material basis for shale gas generation.

CONCLUSION

The geochemical and petrographic analyses of the shale from ZK001 well and ZK2002 well in the Qilian Basin deemed the following conclusions. The organic matter of the shales from ZK001 well and ZK2002 well should be deposited in a marine shelf depositional environment. This conclusion could be enables by various geochemical parameters, such as Pr/Ph; Pr/n-C_{17}, Ph/n-C_{18}, the triangular diagram of the proportion of C_{27}, C_{28}, and C_{29} αα steranes, the gammacerane parameter, the oleanane parameter, the triangular diagram of the proportion of Fs, DBFs, and DBTs in aromatic compounds, and the DBT/P ratio of the aromatics. The high TOC contents of the studied shale include large amounts of vitrinite and sapropelinite, and the organic matters had a highly mature type III kerogen. These conclusions could be enables by the values of various geochemical parameters, such as TOC, KTI, HI, Ro, Tmax, the CPI of the n-alkanes, the sterane C_{29}αα20S/(20S + 20R) and C_{29}ββ/(ββ + αα), the hopane C_{31}22S/(22S + 22R) and Ts/Tm, the MPI and the Rc of the aromatics. The shale samples from ZK001 well and ZK2002 well had very good gas generation potential according to the many of highly mature organic matter of type III (the TOC of 85 and 75% of the samples were greater than 1.0%, respectively).

DATA AVAILABILITY STATEMENT

The original contributions presented in the study are included in the article/supplementary material, further inquiries can be directed to the corresponding author/s.

AUTHOR CONTRIBUTIONS

GW, MS, and HT collected the samples. GW, ZY, and LZ prepared the samples. MS and GW conceived the project, analyzed the samples, and wrote the manuscript. GW, MS, and JY interpreted the data. All authors reviewed the manuscript.

FUNDING

All the experiments were performed at the Geochemistry Analytical & Testing Center, Northwest Institute of Eco-Environment and Resources, Chinese Academy of Sciences. This study was supported by the National Natural Science Foundation of China (Grant No. 41603014) and by a Key Laboratory Project of Gansu Province (Grant No. 1309RTSA041).

REFERENCES

Awan, R. S., Liu, C. L., Gong, H. W., Dun, C., Tong, C., and Chamssidini, L. G. (2020). Paleo-sedimentary environment in relation to enrichment of organic matter of early cambrian black rocks of niutitang formation from xiangxi area China. *Mar. Petroleum Geol.* 112:104057. doi: 10.1016/j.marpetgeo.2019.104057

Chen, J. Z., He, L. X., Liu, L. B., An, S. T., and Shen, J. (2016). An analysis of reservoir conditions and geochemical characteristics of the triassic shale gas in Qilian region, Qinghai Province. *Geol. Bull. China* 35, 273–281.

Cortes, J. E., Niño, J. E., Poloa, J. A., Tobo, A. G., Gonzalez, C., and Siachoquea, S. C. (2013). Molecular organic geochemistry of the Apiay field in the Llanos basin, Colombia. *J. South Am. Earth Sci.* 47, 166–178. doi: 10.1016/j.jsames.2013.07.007

Dai, J. X., Dong, D. Z., Ni, Y. Y., Hong, F., Zhang, S. Y., Zhang, Y. L., et al. (2020). Some essential geological and geochemical issues about shale gas research in China. *Nat. Gas Geosci.* 31, 745–760. doi: 10.11764/j.issn.1672-1926.2020.05.016

El Diasty, W. Sh., Peters, K. E., Moldowan, J. M., Essa, G. I., and Hammad, M. M. (2020). Organic geochemistry of condensates and natural gases in the northwest Nile Delta offshore Egypt. *J. Petroleum Sci. Eng.* 187:106819. doi: 10.1016/j.petrol.2019.106819

El-Sabagh, S. M., El-Naggar, A. Y., Nady, M. M. E., Badr, I. A., Ebiad, M. A., and Abdullah, E. S. (2020). Fingerprinting of biomarker characteristics of some Egyptian crude oils in Northern Western Desert as evidence for organic matter input and maturity level assessment. *Egyptian J. Petroleum* 27, 201–208. doi: 10.1016/j.ejpe.2017.05.004

Fang, R. H., Littke, R., Zieger, L., Baniasad, A., Li, M. J., and Schwarzbauer, J. (2019). Changes of composition and content of tricyclic terpane, hopane, sterane, and aromatic biomarkers throughout the oil window: a detailed study on maturity parameters of Lower Toarcian Posidonia Shale of the Hils Syncline. NW Germany. *Organ. Geochem.* 138:103928. doi: 10.1016/j.orggeochem.2019.103928

Fang, R. H., Wang, T. G., Li, M. J., Xiao, Z. Y., Zhang, B. S., Huang, S. Y., et al. (2016). Dibenzothiophenes and benzo[b]naphthothiophenes: molecular markers for tracing oil filling pathways in the carbonate reservoir of the Tarim Basin. NW China. *Organ. Geochem.* 91, 68–80. doi: 10.1016/j.orggeochem.2015.11.004

Fu, J. H., and Zhou, L. F. (2000). Triassic stratigraphic provinces of the southern Qilian basin and their petro-geological features. *Northwest Geosci.* 21, 64–72.

Gonzaleza, L. D. C., Mastalerzb, M., and Filhoa, J. G. M. (2020). Application of organic facies and biomarkers in characterization of paleoenvironmental conditions and maturity of sediments from the Codó Formation in the west-central part of the São Luís Basin. Brazil. *Int. J. Coal Geol.* 225:103482. doi: 10.1016/j.coal.2020.103482

Guo, S. B., Fu, J. J., Gao, D., Li, H. Y., and Huang, J. G. (2015). Research status and prospects for marine-continental shale gases in China. *Petroleum Geol. Exp.*37, 535–340.

Guo, S. B., and Wang, Y. G. (2013). Shale gas accumulation conditions and exploration potential of Carboniferous Benxi formation in Ordos Basin. *Acta Petrolei Sinica* 34, 445–452. doi: 10.7623/syxb201303004

Guo, Y., Liang, M. L., Wang, Z. X., Zhang, L. Y., Li, H. J., and Li, X. S. (2019). Organic geochemistry and mineral composition characteristics in shales of Niutitang Formation northwestern Hunan. *J. Geomechan.* 25, 392–399.

Hakimi, M. H., and Abdullah, W. H. (2013). Organic geochemical characteristics and oil generating potential of the Upper Jurassic Safer shale sediments in the Marib-Shabowah Basin, western Yemen. *Org. Geochem.* 54, 115–124. doi: 10.1016/j.orggeochem.2012.10.003

He, L. X., Deng, X., Hai, T., Liu, L. B., Yin, H. H., and Li, Q. (2015). The analysis of geochemical characteristic of Triassic hydrocarbon source rocks in Qilian Basin in Qinghai Province. *J. Qinghai University* 33, 78–82. doi: 10.13901/j.cnki.qhwxxbzk.2015.01.016

Holba, A. G., Dzou, L. I., Wood, G. D., Ellis, L., Adam, P., Schaeffer, P., et al. (2003). Application of tetracyclic polyprenoids as indicators of input from fresh-brackish water environments. *Organ. Geochem.* 34, 441–469. doi: 10.1016/S0146-6380(02)00193-6

Hu, T., Pang, X. Q., Jiang, S., Wang, Q. F., Zheng, X. W., Ding, X. G., et al. (2018). Oil content evaluation of lacustrine organic-rich shale with strong heterogeneity: a case study of the Middle Permian Lucaogou Formation in Jimusaer Sag. Junggar Basin, NW China. *Fuel* 221, 196–205. doi: 10.1016/j.fuel.2018.02.082

Huang, H., and Pearson, M. J. (1999). Source rock palaeoenvironments and controls on the distribution of dibenzothiophenes in lacustrine crude oils, Bohai Bay Basin, eastern China. *Organ. Geochem.* 30, 1455–1470.

Huang, Y. J., Bai, Y. B., Sun, B. H., Huang, L., and Huang, C. W. (2020). Characteristics and evaluation of Chang 7 source rock of Yanchang Formation in Fuxianarea. Ordos Basin. *Lithologic Reservoirs* 32, 66–75. doi: 10.12108/yxyqc.20200107

Li, C. C., Sun, S. X., Qiao, J. W., Cao, D. Y., Yang, C., Tan, Q. J., et al. (2015). Coal measures features and mineral resources research orientation in Northern Qinghai-Tibetan Plateau. *Coal Geol. China* 27, 1–6. doi: 10.3969/j.issn.1674-1803.2015.05.01

Li, C. W., Tao, S. Z., Dong, D. Z., and Guan, Q. Z. (2015). Comparison of the formation condition of shale gas between domestic and abroad and favorable areas evaluation. *Nat. Gas Geosci.* 26, 986–1000. doi: 10.00764/j.issn.1672-1926.2015.05.0986

Li, D. L., Li, R. X., Zhu, Z. W., Wu, X. L., Cheng, J. H., Liu, F. T., et al. (2017). Origin of organic matter and paleo-sedimentary environment reconstruction of the Triassic oil shale in Tongchuan City, southern Ordos Basin (China). *Fuel* 208, 223–235. doi: 10.1016/j.fuel.2017.07.008

Li, Y. J., Liu, H., Liu, J. X., Cao, L. C., and Jia, X. C. (2011). Gelolgical regional selection and an evaluation method of resource potential of shale gas. *J. Southwest Petroleum University: Sci. Technol. Ed.* 33, 28–34.

Li, Y. X., Nie, H. K., and Long, P. Y. (2009). Development characteristics of organic-rich shale and strategic selection of shale gas exploration area in China. *Nat. Gas Industry* 29, 115–120.

Liu, C. C., Wang, W. T., Zhang, P. Z., Pang, J. Z., and Yu, J. X. (2016). Magnetostratigraphy and magnetic anisotropy of the Neogene sediments in the Qilian Basin. *Chinese J. Geophys.* 59, 2965–2978. doi: 10.6038/cjg20160820

Liu, M. H., Wang, T. G., Zhong, N. N., Zhang, W. B., Sadik, A., and Li, H. B. (2013). Ternary diagram of fluorenes, dibenzothiophenes and dibenzofurans: indicating depositional environment of crude oil source rocks. *Energy Explorat. Exploitat.* 31, 569–588. doi: 10.1260/0144-5987.31.4.569

Ma, W. X., Liu, S. G., Huang, W. M., Zhang, C. J., Zeng, X. L., and Wang, J. (2012). Basic characteristics of Lower Silurian Longmaxi Formation in in SE margin of Sichuan Basin. *Chinese J. Geol.* 47, 406–421.

Martins, L. L., Schulz, H. M., Ribeiro, H. J. P. S. R., Nascimento, C. A. D., Souza, E. S. D., and Cruz, G. F. D. (2020). Organic geochemical signals of freshwater dynamics controlling salinity stratification in organic-rich shales in the Lower Permian Irati Formation (Paraná Basin. Brazil). *Organ. Geochem.* 140:103958. doi: 10.1016/j.orggeochem.2019.103958

Nie, H. K., Tang, X., and Bian, R. K. (2009). Controlling factors for shale gas accumulation and prediction of potential development area in shale gas reservoir of South China. *Acta Petrolei Sinica* 30, 484–491.

Qian, J., Ma, R. L., Bu, S. F., and Xu, F. H. (2013). Lithofacies-paleogeographical characteristics of marine shale series of strata in Xiangzhong and Xiangdongnan depressions, Huna, China. *J. Chengdu University Technol.* 40, 688–695. doi: 10.969/j.issn.1671-9727.2013.06.08

Radke, M. (1988). Application of aromatic compounds as maturity indicators in source rocks and crude oils. *Mar. Petroleum Geol.* 5, 224–236. doi: 10.1016/0264-8172(88)90003-7

Sousaa, E. D. S., Júniorb, G. R. S., Silvaa, A. F., Reisb, F. D. A. M., Sousaa, A. A. C. D., Cioccaric, G. M., et al. (2019). Biomarkers in cretaceous sedimentary rocks from the Codó Formation - Parnaíba Basin: paleoenvironmental assessment. *J. South Am. Earth Sci.* 92, 265–281. doi: 10.1016/j.jsames.2019.03.025

Su, Y. F., Zhang, Q. H., and Wei, Z. C. (2016). Permo-Carboniferous shale gas resources potential assessment in Qinshui Basin. *Coal Geol. China* 28, 27–34. doi: 10.3969/j.issn.1674-1803.2016.04.06

Sun, J., Zheng, Q. G., Wen, Z. H., Hou, F. H., Xiao, R., and Ren, J. Z. (2014). Shale gas reservoir-forming conditions and exploration prospect in Permian Shanxi Formation of the Southern North China Basin. *Mar. Geol. Front.* 30, 20–28. doi: 10.16028/j.1009-2722.2014.04.006

Tao, S., Tang, D. Z., Xu, H., Liang, J. L., and Shi, X. F. (2013). Organic geochemistry and elements distribution in Dahuangshan oil shale, southern Junggar Basin: origin of organic matter and depositional environment. *Int. J. Coal Geol.* 115, 41–51. doi: 10.1016/j.coal.2013.05.004

Tuo, J. C., Wu, C. J., and Zhang, M. F. (2016). Organic matter properties and shale gas potential of Paleozoic shales in Sichuan Basin. China. *J. Nat. Gas Sci. Eng.* 28, 434–446. doi: 10.1016/j.jngse.2015.12.003

Wang, G. C., Sun, M. Z., Gao, S. F., and Tang, L. (2018). The origin, type and hydrocarbon generation potential of organic matter in a marine-continental transitional facies shale succession (Qaidam Basin. China). *Sci. Rep.* 6568:6568. doi: 10.1038/s41598-018-25051-1

Wang, L., Zhou, L. F., and Li, S. (2013). Reservoir characteristics and comprehensive evaluation of Triassic clastic reservoir in southern Qilian Basin. *J. Hebei University Eng.* 30, 65–70.

Wang, T., Li, L., Li, D. L., Yang, Y. J., Ma, L. Y., Pang, Y. C., et al. (2011). Characteristics of biomarkers of the black rock series of lower cambrian niutitang formation in the nayong area, western guizhou, China. *Geol. Bull. China* 30, 106–111.

Zhang, J. Z., Li, X. Q., Liu, Y., Cai, Y. Q., Wang, Y., Niu, H. Y., et al. (2015). Longtan formation shale gas reservoiring conditions and favorable region analysis in southern sichuan area. *Coal Geol. China* 26, 1–6. doi: 10.3969/j.issn.1674-1803.2014.12.01

Zhang, W., Guan, P., Han, D. K., Meng, Q. X., Xie, X. Q., Jian, X., et al. (2013). Evaluation of terrestrial hydrocarbon source rocks and oil source correlation in triassic and jurassic in Northeastern sichuan. *Acta Scientiarum Naturalium Universitatis Pekinensis* 49, 826–838. doi: 10.13209/j.0479-8023.2013.111

Zou, C. N., Dong, D. Z., Wang, S. J., Li, J. Z., Li, X. J., Wang, Y. M., et al. (2010). Geological characteristics, formation mechanism and resource potential of shale gas in China. *Petroleum Explorat. Dev.* 37, 641–653.

Zumberge, J., Ferworn, K., and Brown, S. (2012). Isotopic reversal ('rollover') in shale gases produced from the mississippian barnett and fayetteville formations. *Mar. Petroleum Geol.* 31, 43–52. doi: 10.1016/j.marpetgeo.2011.06.009

Conflict of Interest: LZ was employed by the company PetroChina.

The remaining authors declare that the research was conducted in the absence of any commercial or financial relationships that could be construed as a potential conflict of interest.